

## A further crystal structure refinement of gersdorffite

PETER BAYLISS

Department of Geology and Geophysics  
University of Calgary, Alberta T2N 1N4, Canada

### Abstract

Thirteen gersdorffite (NiAsS) specimens were analyzed with electron microprobe, powder diffraction, and precession camera techniques. For each specimen, a sample with a well-developed cube form {100} was selected. Intensity data were collected from 27 reflections, which are mostly forbidden by cubic space group  $Pa\bar{3}$ , with a single crystal diffractometer. X-ray powder diffraction data indicate two pyrite subgroup specimens, five ullmannite subgroup specimens, and six cobaltite subgroup specimens. A complete intensity data set was collected by single crystal diffractometer from three of these six cobaltite subgroup samples. Least-squares refinement shows different degrees of apparent As–S disorder with one sample significantly ordered (predominantly three twin-related domains) and the other two samples disordered (equal amounts of six twin-related domains). These three crystal structures are similar to those described for cobaltite. They are explained as a sextuplet of orthorhombic ( $Pca2_1$ ) interpenetrating twin-related domains about a  $\bar{3}$  twin axis [111].

Although the chemical compositions of the three different pyrite-type crystal structures overlap, there is a tendency for the two pyrite subgroup (true As–S disorder at the atomic level,  $Pa\bar{3}$ ) specimens to contain more As, and a tendency for the six cobaltite subgroup (true As–S order at the atomic level,  $Pca2_1$ ) specimens to contain more Co and Fe than the five ullmannite subgroup (true As–S order at the atomic level,  $P2_1\bar{3}$ ) specimens. These three crystal structures are probably temperature dependent with  $P2_1\bar{3}$  the low form,  $Pca2_1$  the intermediate (metastable?) form, and  $Pa\bar{3}$  the high form.

### Introduction

Three crystal structure variants of gersdorffite have been described as follows: an ordered pyrite-type structure ( $P2_1\bar{3}$ , ullmannite subgroup, Bayliss and Stephenson, 1967); a disordered pyrite-type structure ( $Pa\bar{3}$ , pyrite subgroup, Bayliss 1968); and a distorted disordered pyrite-type structure ( $P1$ , gersdorffite III, Bayliss and Stephenson, 1968). An alternative interpretation to these diffraction data for gersdorffite III is suggested by the work of Bayliss (1982), who interprets different As–S order-disorder within cobaltite crystals as a sextuplet of orthorhombic ( $Pca2_1$ ) interpenetrating twin-related domains about a  $\bar{3}$  twin axis [111]. In view of this, the crystal structure of gersdorffite III is re-examined in more detail.

The 010 and 110 reflections may be used to differentiate between space groups  $Pca2_1$ ,  $P2_1\bar{3}$  and  $Pa\bar{3}$ . Berry and Thompson (1962) did not observe the 010 and 110 reflections in gersdorffite, (Ni,Fe,Co)AsS, from Sudbury, Ontario (ROM M12176 and

ROM M15861) with Straumanis-type powder photographs, Cu radiation and Ni filter. They state “pattern similar to that of cobaltite”, although they observed the 010 and 110 reflections in cobaltite from Hakensbo. These weak 010 and 110 reflections are difficult to observe, since they may be hidden by the high background fluorescence from the Fe and Co in gersdorffite with Cu radiation. These 010 and 110 reflections were observed in both Debye-Scherrer photographs and powder diffractometer patterns in six gersdorffite specimens (USNM R830, BM1922,145, USNM R862, BM1929,12, HMM, BM57562) by Bayliss (1969a).

Klemm (1962), Ramdohr (1969), and Cabri and Laflamme (1975) indicate that most specimens of gersdorffite are optically isotropic, but some are optically anisotropic. Bayliss (1969a) shows a gradual increase from optically isotropic for NiAsS to the strongest optical anisotropy for CoAsS in the gersdorffite–cobaltite solid solution series. Optical anisotropy is most frequently recognized by Klemm (1962) through twin lamellae after {111}? and {100}.

Ramdohr (1969) states "all authentic specimens examined by the writer or by Meyer (1926) did not exhibit lamellar structure", however, Bayliss (1969a) observed twinning in gersdorffite from Leichtenberg (USNM R862) and Lobenstein (BM57562).

### Experimental and results

Thirteen gersdorffite specimens were obtained for this investigation from the British Museum (BM), Royal Ontario Museum (ROM), United States National Museum (USNM), and University of New South Wales (UNSW). The specimens, which have previously been studied, are BM 1434, BM 57562, BM 1917,285, BM 1922,145, BM 1929, 12, BM 1933,371, BM 1959,462, USNM R862 and UNSW by Bayliss (1969a), and ROM M12176 and ROM M15861 by Berry and Thompson (1962). Specimen numbers with their localities are listed in Table 1, and the same order is also used in Tables 2 and 3.

Powder diffractometer patterns may be divided into three groups as follows: (1) both the 010 and 110 reflections are observed in six gersdorffite specimens (57562, R862, 1929,12, M12176, M15861, and 1922,145), (2) the 010 reflection is absent although the 110 reflection is observed in five gersdorffite specimens (1959,462, 113044, 1434, 120381, and 1917,285), and (3) reflections 010 and 110 are absent in two gersdorffite specimens (1933,371 and UNSW). The shapes of reflections 010 and 110 are similar to those of the other reflections recorded. The presence of these 010 and 110 reflections have been confirmed by 114.6 mm Debye-Scherrer powder photographs. Neither powder diffractometer patterns nor Debye-Scherrer powder photographs

Table 2. Electron microprobe analyses

| Specimen Number | Fe  | Co   | Ni   | S    | As   | Sb  | Total |
|-----------------|-----|------|------|------|------|-----|-------|
| NiAsS           |     |      | 35.4 | 19.4 | 45.2 |     | 100.0 |
| 57562           | 0.2 | 0.2  | 34.1 | 17.8 | 46.7 | 0.1 | 99.1  |
| R862            | 1.8 | 0.7  | 32.9 | 18.8 | 45.0 | 0.4 | 99.6  |
| 1929,12         | 2.3 | 0.5  | 32.1 | 19.2 | 44.7 | 0.2 | 99.0  |
| M12176          | 5.3 | 5.4  | 23.6 | 18.2 | 46.6 | 0.1 | 99.2  |
| M15861          | 6.5 | 9.3  | 18.8 | 18.7 | 46.8 | 0.3 | 100.4 |
| 1922,145        | 1.7 | 17.8 | 14.8 | 16.2 | 50.0 |     | 100.5 |
| 1959,462        | 0.4 | 0.3  | 34.1 | 18.3 | 44.5 | 1.5 | 99.1  |
| 113044          | 0.9 | 1.2  | 33.6 | 20.0 | 45.4 |     | 101.1 |
| 1434            | 1.0 | 1.4  | 32.6 | 18.9 | 43.6 | 1.7 | 99.2  |
| 120381          | 0.6 | 4.2  | 27.6 | 11.0 | 57.5 |     | 100.9 |
| 1917,285        | 5.6 | 0.1  | 29.3 | 17.1 | 48.7 | 0.1 | 100.9 |
| UNSW            | 1.3 | 0.4  | 32.0 | 14.2 | 52.5 | 0.4 | 100.8 |
| 1933,371        | 3.3 | 2.2  | 26.3 | 10.1 | 58.0 | 0.8 | 100.7 |

showed distinct reflection splitting. Most specimens of groups (2) and (3) above show sharp reflections near  $\theta = 90^\circ$ , which indicates cubic symmetry. On the other hand, most specimens of group (1) above show broad reflections near  $\theta = 90^\circ$ , which may be interpreted as multiple reflections from a pseudocubic mineral.

All gersdorffite specimens were chemically analyzed by electron microprobe as previously described by Bayliss (1982). Calculation of the stoichiometry from electron microprobe results in Table 2 based upon a  $4MX_n$  structural formula indicates that  $n$  varies between 1.97 and 2.03. Since the electron microprobe data contain random errors, no evidence is available to indicate deviations from stoichiometric  $MX_2$ . The Ni-As-S system described by Yund (1962) gives a  $MX_2$  formula for gersdorffite based upon chemical syntheses and a literature survey. A similar conclusion has been deduced by Klemm (1965). Therefore it appears logical to accept a stoichiometric  $MX_2$  formula.

The gersdorffite specimens (Table 2) show a wide range of substitution of Ni by Co and Fe, which falls within the solid solution limits of the ternary diagram FeAsS-CoAsS-NiAsS at 500° C of Klemm (1965). Metal chemical zoning is observed in specimen M12176, where a 9% Ni variation is inversely proportional to a 2% Fe and 7% Co variation. The specimens also show a wide range of substitution of S by As, which falls within the solid solution limits of Yund (1962) at 450° C. Non-metal chemical zoning is observed in specimen UNSW, where a 9% As variation is inversely proportional to a 4% S variation.

Table 1. Specimen numbers and their localities

| Specimen Number | Locality                              |
|-----------------|---------------------------------------|
| BM 57562        | Lobenstein, Russ, Germany             |
| USNM R862       | Leichtenberg, Fichtelgebirge, Germany |
| BM 1929,12      | Mitterburg, Salzburg, Austria         |
| ROM M12176      | Crean Hill, Sudbury, Ont., Canada     |
| ROM M15861      | Garson Mine, Sudbury, Ont., Canada    |
| BM 1922,145     | Cobalt, Ont., Canada                  |
| BM 1959,462     | Cochabamba, Bolivia                   |
| USNM 113044     | Temagami, Ont., Canada                |
| BM 1434         | Musen, Westphalia, Germany            |
| USNM 120381     | Art Ahmane, Bou Azzer, Morocco        |
| BM 1917,285     | Sudbury, Ont., Canada                 |
| UNSW            | Ferro, Slovakia, Czechoslovakia       |
| BM 1933,371     | Farvic Mine, Gwanda, Rhodesia         |

From each gersdorffite specimen, a sample was selected with an approximately equidimensional well-developed cube form {100}. The preliminary alignment along an *a* axis was made on a precession camera using unfiltered Mo radiation. These precession photographs *hk0* and *h0l* confirmed the presence of reflections 010 and 110 observed in the powder diffractometer patterns. Simple twinning was not observed by either reflection splitting or the presence of strong 210 and strong 120 reflections. Strong 210 and 120 reflections may result from a (110) twin plane as shown by iron cross twinning in pyrite (Tennyson, 1980). The observed reflection intensities (*I*) within each of the three groups defined by the powder diffractometer patterns are similar, except for M15861 where  $I_{010} > I_{001} > I_{100}$  whereas for all other samples in this group  $I_{010} = I_{001} = I_{100}$ . Similar results were obtained from precession photographs of additional samples from these gersdorffite specimens.

Eight of these gersdorffite samples were selected for single crystal diffractometry. Each sample was accurately centered on a manual four circle diffractometer with reflections 800,  $\bar{8}00$  and 080 so that an *a* axis coincided with the diffractometer  $\phi$  axis. Integrated intensities of 27 reflections, which in-

cludes 24 reflections forbidden by space group *Pa3*, were collected. These integrated intensities were corrected for background and scaled so that the maximum observed relative intensity (*I*) is 1000. Values of 1 are approximately equal to the limit of detection at the  $3\sigma$  confidence level.

The crystallographic axes of each sample were chosen so that  $I_{120} \gg I_{210}$ , and if possible  $I_{010} > I_{001} > I_{100}$ . This is satisfied by only one of the six possible orthogonal orientations. If  $I_{010} = I_{001} = I_{100}$ , then three different orthogonal orientations are possible. Each column of Table 3 has been arranged in sets of three reflections, which are equivalent in the cubic space groups *P2<sub>1</sub>3* and *Pa3*. The observed relative intensities (*I*) of the nine samples, which are given in Table 3, have been arranged so that samples with similar intensities are grouped together. The values of  $F_{201}$ ,  $F_{120}$  and  $F_{012}$  recorded in Table 4 for two gersdorffite samples are approximately equal. The variability between the values of  $I_{201}$ ,  $I_{120}$  and  $I_{012}$  in Table 3 for eight gersdorffite samples is by a factor of about three, which takes into account the fact that these observed relative intensities have not been corrected for absorption. Therefore for these gersdorffite samples, the relative intensity of a reflection from one sample must be at least triple the relative intensity of the same reflection from another sample to be considered different. With this limitation, Table 3 confirms the results (three groups) obtained from powder diffraction patterns and precession camera photographs so that it is not essential to correct all the relative intensities for absorption and calculate their standard deviations.

In specimen 1933,371, reflections 010 and 110 are absent in a powder diffractometer pattern, Debye-Scherrer photograph and precession camera photographs. A number of weak reflections are recorded in Table 3, which are systematically absent in space group *Pa3* after the crystallographic axes are rotated to *yxz* to produce Miller indices of *hkl* in Table 3. These weak reflections have a different shape compared to the other reflections. Similar weak reflections, which have been attributed to the Renninger effect, have been observed in pyrite-type crystal structures in space group *Pa3* by Pratt and Bayliss (1979) and King and Prewitt (1980). Therefore the crystal structure of 1933,371 is similar to the gersdorffite (disordered, *Pa3*, pyrite subgroup) of Bayliss (1968).

In four specimens (1917,285, 120381, 1434, and 113044), the 010 reflection is absent in the powder

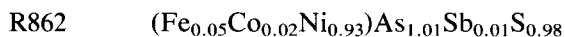
Table 3. Observed relative intensities from eight gersdorffite samples

| <i>hkl</i> | <i>Pa2<sub>1</sub></i> |            |            |       | <i>P2<sub>1</sub>3</i> |      |             |              | <i>Pa3</i>   |
|------------|------------------------|------------|------------|-------|------------------------|------|-------------|--------------|--------------|
|            | *<br>R862              | *<br>12176 | *<br>15861 | 15861 | 113-<br>044            | 1434 | 120-<br>381 | 1917,<br>285 | 1933,<br>371 |
| 010        | 12                     | 70         | 132        | 15    | 5                      | 0    | 6           | 5            | 3            |
| 001        | 15                     | 35         | 37         | 1     | 0                      | 0    | 1           | 4            | 1            |
| 100        | 12                     | 23         | 36         | 3     | 1                      | 0    | 1           | 0            | 2            |
| 030        | 3                      | 20         | 27         | 11    | 0                      | 0    | 0           | 0            | 0            |
| 003        | 10                     | 13         | 7          | 1     | 3                      | 1    | 3           | 0            | 1            |
| 300        | 4                      | 7          | 7          | 1     | 0                      | 0    | 0           | 1            | 0            |
| 050        | 5                      | 19         | 24         | 12    | 4                      | 0    | 7           | 1            | 3            |
| 005        | 6                      | 13         | 8          | 1     | 0                      | 0    | 0           | 3            | 0            |
| 500        | 3                      | 11         | 10         | 5     | 1                      | 0    | 1           | 0            | 0            |
| 070        | 4                      | 12         | 15         | 8     | 0                      | 0    | 1           | 0            | 0            |
| 007        | 4                      | 8          | 5          | 1     | 0                      | 0    | 0           | 0            | 0            |
| 700        | 4                      | 6          | 4          | 1     | 0                      | 0    | 0           | 0            | 0            |
| 110        | 69                     | 25         | 53         | 10    | 130                    | 99   | 95          | 121          | 0            |
| 011        | 32                     | 29         | 16         | 1     | 176                    | 110  | 131         | 121          | 0            |
| 101        | 31                     | 33         | 13         | 2     | 22                     | 18   | 26          | 58           | 0            |
| 120        | 1000                   | 371        | 1000       | 1000  | 1000                   | 1000 | 956         | 1000         | 909          |
| 012        | 670                    | 1000       | 667        | 370   | 986                    | 937  | 1000        | 837          | 1000         |
| 201        | 663                    | 610        | 900        | 371   | 226                    | 263  | 311         | 484          | 370          |
| 210        | 87                     | 5          | 4          | 1     | 151                    | 119  | 115         | 224          | 0            |
| 021        | 65                     | 10         | 1          | 1     | 315                    | 225  | 240         | 241          | 0            |
| 102        | 44                     | 11         | 1          | 1     | 44                     | 26   | 45          | 106          | 0            |
| 310        | 18                     | 8          | 17         | 6     | 23                     | 20   | 20          | 54           | 1            |
| 031        | 20                     | 11         | 5          | 1     | 76                     | 54   | 59          | 54           | 0            |
| 103        | 12                     | 16         | 4          | 1     | 13                     | 7    | 11          | 29           | 0            |
| 130        | 14                     | 10         | 19         | 7     | 45                     | 32   | 35          | 34           | 2            |
| 013        | 11                     | 11         | 5          | 1     | 43                     | 29   | 41          | 24           | 0            |
| 301        | 8                      | 7          | 5          | 1     | 15                     | 13   | 16          | 19           | 0            |

diffractometer pattern, Debye-Scherrer photograph and precession camera photographs, although the 110 reflection is observed. A number of weak reflections ( $h00$ ,  $0k0$ , and  $00l$ ) are recorded in Table 3, which are systematically absent in space group  $P2_13$ . These weak reflections have a different shape compared to the other reflections. Similar weak reflections, which have been attributed to the Renninger effect, have been observed in pyrite-type crystal structures in space group  $P2_13$  by Pratt and Bayliss (1980). Therefore the crystal structure of these four specimens is similar to the gersdorffite (ordered,  $P2_13$ , ullmannite subgroup) of Bayliss and Stephenson (1967).

Three specimens (R862, M12176 and M15861) have no systematic absences, and reflections 010 and 110 are also observed in a powder diffractometer pattern, Debye-Scherrer photograph and precession camera photographs. The four samples have been arranged from left to right across Table 3 with  $I_{010} = I_{001} = I_{100}$  (distorted and disordered crystal structure of Bayliss and Stephenson, 1968) to  $I_{010} \gg I_{001} = I_{100}$  (cobaltite-low ordered crystal structure in  $Pca2_1$  of Giese and Kerr, 1965). Reflections that would be extinct in the untwinned crystal structure with space group  $Pca2_1$  are 001, 100, 011, 101, 031, 103, 013, 301, 033 and 303.

In order to investigate the crystal structure of gersdorffite further, specimen R862 ( $I_{010} = I_{001} = I_{100}$ ) was again selected together with M12176 ( $I_{010} > I_{001} > I_{100}$ ) and M15861 ( $I_{010} \gg I_{001} = I_{100}$ ) for single crystal structure analysis. These are marked by \* in Table 3. The second sample of M15861 could not be used, because it has an irregular shape. Their derived chemical formulae based upon a  $4MX_2$  structural formulae are as follows:



All reflections, which were recorded by powder diffractometer patterns, Debye-Scherrer and precession photographs, may be indexed on a cubic unit cell with  $a$  between 5.63 and 5.71 Å. Cubic unit cells were calculated from Debye-Scherrer photographs by the Nelson and Riley (1945) extrapolation method to  $\theta = 90^\circ$ . A comparison of these cubic unit cells with 5.693 Å of NiAsS (Yund, 1962) and 5.576 Å of CoAsS (Bayliss, 1969b) and also with the chemical analyses in Table 2 confirms that Co decreases the cubic unit cell and As increases the

Table 4. Structure factors from two gersdorffite samples

| $hkl$ | M15861    |            | M12176    | $hkl$ | M15861    |            | M12176    |
|-------|-----------|------------|-----------|-------|-----------|------------|-----------|
|       | $F_{obs}$ | $F_{calc}$ | $F_{obs}$ |       | $F_{obs}$ | $F_{calc}$ | $F_{obs}$ |
| 100   | 11.7      | 2.7        | 6.3       | 201   | 97.0      | 93.2       | 104.5     |
| 010   | 24.2      | 22.6       | 8.1       | 120   | 96.7      | 92.7       | 100.5     |
| 001   | 15.3      | 12.0       | 8.3       | 012   | 94.0      | 89.1       | 110.1     |
| 300   | 8.8       | 3.1        | 9.7       | 102   | 1.8       | 4.7        | 2.3       |
| 030   | 18.9      | 18.5       | 5.9       | 210   | 5.4       | 4.3        | 2.9       |
| 003   | 11.4      | 11.6       | 7.7       | 021   | 3.7       | 3.7        | 3.0       |
| 500   | 14.6      | 6.7        | 11.3      | 103   | 7.4       | 4.4        | 5.5       |
| 050   | 24.6      | 21.7       | 9.1       | 310   | 14.8      | 12.9       | 5.2       |
| 005   | 15.3      | 9.5        | 15.1      | 031   | 10.2      | 9.9        | 7.1       |
| 700   | 11.2      | 10.2       | 11.7      | 301   | 8.1       | 5.4        | 6.4       |
| 070   | 24.0      | 21.4       | 9.0       | 130   | 15.5      | 12.2       | 5.6       |
| 007   | 14.6      | 11.5       | 11.1      | 013   | 9.6       | 10.1       | 9.2       |
| 101   | 9.4       | 2.4        | 5.6       | 303   | 13.1      | 2.8        | 8.1       |
| 110   | 17.5      | 19.6       | 5.1       | 330   | 18.3      | 18.0       | 7.2       |
| 011   | 11.6      | 4.8        | 6.0       | 033   | 11.8      | 7.5        | 15.6      |

cubic unit cell. Cubic unit cell differences between samples of the same specimen are attributed to the Ni:Fe+Co or As:S chemical zoning. For each of the three gersdorffite samples, the angular position of about 20 strong reflections at high  $2\theta$  values were measured. No deviation was detectable from  $a = b = c$  and  $\alpha = \beta = \gamma = 90^\circ$ . These measurements yielded  $a = 5.622(3)\text{Å}$  for M15861,  $a = 5.657(3)\text{Å}$  for M12176, and  $a = 5.685(3)\text{Å}$  for R862.

Integrated intensities of all reflections from one hemisphere were collected with  $\text{MoK}\alpha$  radiation and a graphite 002 monochromator. For M15861, 1151 reflections within the range  $5^\circ < 2\theta < 65^\circ$  were scanned twice in a  $\theta:2\theta$  mode at  $1^\circ 2\theta$  per minute over the scan width of  $1.9^\circ + \text{btan } \theta$ . For M12176, 1017 reflections within the range  $5^\circ < 2\theta < 60^\circ$  were scanned in a  $\theta:2\theta$  mode at  $1/2^\circ 2\theta$  per minute over the scan width of  $1.7^\circ + \text{btan } \theta$ . For R862, about 2000 reflections within the range  $5^\circ < 2\theta < 80^\circ$  were step scanned twice in a  $\theta:2\theta$  mode at a  $0.01:0.02^\circ 2\theta$  step after each second over the scan width of  $2.4^\circ 2\theta$ . Background counts were measured for ten seconds at both the beginning and end of each reflection measurement. A standard 020 reflection, which was measured every 50 reflections throughout the data collection, showed satisfactory experimental stability, so that no correction was applied for instrumental drift.

Background, Lorenz, polarization, and absorption corrections were made following the method of Wuensch and Prewitt (1965). The sample from M15861 measured  $108(3)\text{ }\mu\text{m} \times 44(3)\text{ }\mu\text{m} \times 30(3)$

$\mu\text{m}$  and has a linear absorption coefficient of  $313\text{ cm}^{-1}$ . Transmission factors of 0.36 to 0.51 were calculated from an absorption correction based upon 240 grid points arranged in a gaussian distribution. This absorption correction was checked by the measurement of both the 010 and 080 reflections at every  $10^\circ\phi$  about the scattering vector by a  $\theta:2\theta$  scan to give 36 different measurement positions for both reflections. These  $F_{\text{obs}}$  values are consistent to  $\pm 4\%$ , and their reflection shapes are similar to those of other reflections so that these reflections are not caused by the Renninger effect. The sample from M12176 measured  $156(3)\ \mu\text{m} \times 84(3)\ \mu\text{m} \times 124(2)\ \mu\text{m}$  and has a linear absorption coefficient of  $309\text{ cm}^{-1}$ . Transmission factors of 0.05 to 0.12 were calculated from an absorption correction based upon 960 grid points arranged in a gaussian distribution.

The observations of reflections forbidden by space group  $Pca2_1$  may be explained by either complex twinning or further ordering of the Fe, Co, Ni, As, Sb and S atoms among the twelve sites. In order to investigate these possibilities, least-squares refinement was undertaken with the procedure described by Bayliss (1982) and with the initial positional parameters from Bayliss (1968). The  $\text{Sb}_{0.01}$  in M15861 was placed in site  $X_6$ , because site  $X_6$  indicated the most atomic scattering power. For M15861, the resultant  $R$  value was 0.08 in space group  $P1$  with the Fe, Co and Ni evenly distributed about the four metal sites. Sample M15861 was not refined in space group  $Pca2_1$ , because the structure factors of  $0kl$  with  $l$  odd and  $h0l$  with  $h$  odd, which are forbidden in space group  $Pca2_1$ , are clearly observable in Table 5. The strong correlation between site occupancies and temperature factors for M12176 means that site occupancy refinement was not possible. Therefore the As and S were evenly distributed among the eight non-metal sites (X) and the Fe, Co and Ni were evenly distributed among the four metal sites (M). Individual temperature

factors were varied to seek potential differences between similar sites. For M12176, the resultant  $R$  value in space group  $P1$  was 0.09.

### Discussion

The positional parameters of atoms for M12176 and M15861 in space group  $Pca2_1$  are  $\text{M}(0,1/4,0)$ ,  $\text{X}(3/8,5/8,3/8)$  and  $\text{X}(5/8,7/8,5/8)$ . Only one of the six orthogonal orientations is possible for M15861, but three orthogonal orientations are possible for M12176. These positional parameters are then similar to those generated by space group  $Pa3$  after reduction by the vector  $(0, -1/4, 0)$  with axes  $yxz$  and atoms of  $\text{M}(0,0,0)$  and  $\text{X}(3/8,3/8,3/8)$ .

Since the second sample of R862 gave a similar crystal structure refinement to that reported by Bayliss and Stephenson (1968), the refinement method is not repeated. The  $R$  value of 0.15 in space group  $P1$  is lower than the previous determination of 0.19. Since this result has been repeated, it appears consistent, although the crystal structure model is incorrect because the  $R$  value is too high.

The strong correlation between site occupancies and temperature factors for M12176 indicates that site occupancy refinement is not possible. If site ordering does occur, it would be reflected by large temperature factor differences. Since the temperature factors of  $\text{M}_1$  to  $\text{M}_4$  and  $\text{X}_1$  to  $\text{X}_8$  lie with  $3\sigma$ , it is concluded that neither metal nor non-metal site ordering can be observed. The crystal structure of M12176 is similar to that of R862, and is also consistent with the earlier work of Bayliss and Stephenson (1968).

The crystal structures of R862 and M12176 are similar to the crystal structure of cobaltite D37829 (equal amounts of twin-related domains) as described by Bayliss (1982). In addition the least-squares refinements of these three crystal structures of gersdorffite have similar unsatisfactory features of high  $R$  values and strong correlation. A twin analysis of M12176 and R862 may be undertaken, since Bayliss (1969a) observed that specimen R862 is twinned. This twin analysis indicates similar amounts (15 to 20%) of all six orientations from Bayliss (1982) because  $F_{hk0} \approx F_{0kl} \approx F_{h0l}$  (Table 4) and As ordering was not detected in the non-metal sites.

The total amount of As for M15861 in the four non-metal sites (Table 5) related by  $Pca2_1$  symmetry of  $\text{X}_1$  to  $\text{X}_4$  (0.95 As atoms) is significantly less than that in sites  $\text{X}_5$  to  $\text{X}_8$  (3.21 As atoms). Therefore this gersdorffite crystal appears to be signifi-

Table 5. Site occupancies of M15861

| Atom  | S    | As      | Sb   |
|-------|------|---------|------|
| $X_1$ | 0.68 | 0.32(4) |      |
| $X_2$ | 1.0  |         |      |
| $X_3$ | 0.78 | 0.22(5) |      |
| $X_4$ | 0.59 | 0.41(5) |      |
| $X_5$ | 0.32 | 0.68(5) |      |
| $X_6$ |      | 0.99(5) | 0.01 |
| $X_7$ | 0.09 | 0.91(5) |      |
| $X_8$ | 0.38 | 0.62(5) |      |

cantly ordered. The As occupancy sequence of the eight non-metal sites is  $X_7 = X_6 > X_5 = X_8 > X_4 = X_1 > X_3 > X_2$ . This As occupancy sequence correlates with the average interatomic distances, since the longer average interatomic distances correlate with the higher As site occupancies. Also this As occupancy sequence generally correlates with the temperature factors, since the lower temperature factors correlate with the higher As site occupancies. Exceptions to this As occupancy sequence indicated by both average interatomic distances and temperature factors are that  $X_1$  should contain slightly more As, whereas  $X_5$  should contain slightly less As.

The occupancies of the four metal sites for M15861 were refined because there may be a chemical reason for this type of As-S ordering, however no meaningful refinement was expected, because the atomic scattering factors of Fe, Co and Ni are similar. The average interatomic distances about the octahedral metal sites are not only affected by the substitution of Fe and Co for Ni, but also by the amount of As in the six non-metal sites coordinated with each octahedral metal site. The total number of As atoms (Table 5) in these six non-metal sites coordinated with each octahedral metal site are 3.16(30) around  $M_1$ , 3.16(29) around  $M_2$ , 3.03(29) around  $M_3$ , and 3.13(29) around  $M_4$ . An overall analysis of the metal site occupancy refinement, temperature factors, average interatomic distances, and total number of As atoms in the six non-metal sites coordinated with each octahedral metal site shows no systematic trend. Therefore the Fe and Co are randomly distributed among the four metal sites.

The pyrite-type crystal structure may be described as similar to the halite crystal structure, where the metal atom (M) replaces Na and the non-metal pair ( $X_2$ ) replaces Cl. A summation of the As atoms in the non-metal pair ( $X_2$ ) of M15861 from Table 5 gives  $X_1 + X_5 = 1.00(9)$ ,  $X_2 + X_6 = 1.00(10)$ ,  $X_3 + X_7 = 1.13(10)$ , and  $X_4 + X_8 = 1.03(10)$ , so that each non-metal pair contains about one As atom. The interatomic distances between these non-metal pair sites are similar.

The average interatomic angles of M15861 indicate that the coordination of the non-metal atoms has been distorted from a regular tetrahedron ( $109^\circ$  angles) to a trigonal pyramid with average interatomic angles of  $102^\circ$  (M-X-X) and  $116^\circ$  (M-X-M). The coordination of the metal atoms has been distorted from a regular octahedron ( $90^\circ$  angles) to a

trigonal prism with average interatomic angles of  $85^\circ$  ( $X_A$ -M- $X_A$  or  $X_B$ -M- $X_B$ ) and  $95^\circ$  ( $X_A$ -M- $X_B$ ). The  $X_A$  atoms occupy the S sites and the  $X_B$  atoms occupy the As (or Sb) sites in the  $P2_13$  ordering that occurs in gersdorffite (Bayliss and Stephenson, 1967) and ullmannite (Pratt and Bayliss, 1980).

This crystal structure of M15861 is similar to the crystal structure of cobaltite D24919 (predominantly three twin-related domains) as described by Bayliss (1982). A similar twin analysis of M15861 indicates that  $F_{hko} > F_{okl} > F_{hol}$  (Table 4), and three twin orientations (II, III, and V of Bayliss, 1982) are not possible, because As is absent from non-metal site  $X_2$  (Table 5). The results calculated by these two methods are similar with 50% of orientation I, 30% of orientation VI, and 20% of orientation IV.

Heating experiments on six gersdorffite specimens at  $550^\circ$  and  $600^\circ$  C for one week by Bayliss (1969a) indicate a crystal structure change with the loss of the 010 reflection first, and then the loss of the 110 reflection later as detected with powder X-ray diffraction patterns. From these heating experiments, it seems likely that  $P2_13$  is the low temperature ordered phase, whereas  $Pca2_1$  is an intermediate (metastable?) phase, and  $Pa3$  is the high temperature disordered phase. The disappearance of the  $\bar{3}$  axis in the transformation from  $P2_13$  to  $Pca2_1$  requires two of the four fully ordered As pairs to reorient by  $180^\circ$ .

### Conclusions

Similar to cobaltite, these non-cubic crystal structures of gersdorffite are a sextuplet of orthorhombic ( $Pca2_1$ ) interpenetrating twin-related domains about a  $\bar{3}$  twin axis [111]. This explains (1) the trend to higher  $R$  values from apparently significantly ordered (M15861) to apparently disordered (M12176, R862); (2) why the  $R$  value of the disordered crystal structure is above 0.03; (3) the presence of strong reflections forbidden by the disordered crystal structure ( $Pa3$ ); (4) why different samples from M151861 may have different intensities; and (5) why the non-metal site occupancies of the apparently disordered crystal structure do not refine. Therefore the refinement of the crystal structure model in space group  $P1$  is unjustified.

The poor quality of these three crystal structure refinements is attributed to twinning; since the atomic positional parameters of the six orthorhombic orientations are slightly different, because neither  $x$ ,  $y$  and  $z$ , nor  $a$ ,  $b$ , and  $c$  are exactly equal. Systematic errors caused by twinning indicate that

the standard deviations of the positional parameters, and hence also of the interatomic distances and angles, are underestimated. Although it is possible to refine crystal structure models based on twinned crystals, such a refinement is unlikely to provide an excellent quality refinement, because the exact values of  $a$ ,  $b$  and  $c$  are unknown. Therefore a single crystal without twinning should be used to obtain an excellent quality refinement of non-cubic gersdorffite in  $Pca2_1$ .

Although the chemical compositions (Table 2) of the three different crystal structures overlap, there is a tendency for the two pyrite subgroup (true As–S disorder at the atomic level,  $Pa3$ ) specimens to contain more As and a tendency for the six cobaltite subgroup (true As–S order at the atomic level,  $Pca2_1$ ) specimens to contain more Co and Fe than the five ullmannite subgroup (true As–S order at the atomic level,  $P2_13$ ) specimens. Separate species names for all three crystal structures are not necessary, because they are minor derivatives of the pyrite-type crystal structure based upon different types of As–S ordering, which are probably temperature dependent with  $P2_13$  the low form,  $Pca2_1$  the intermediate (metastable?) form, and  $Pa3$  the high form.

#### Acknowledgments

Financial assistance was provided by the Natural Sciences and Engineering Research Council Canada. Mr. B. Rutherford and Mrs. J. L. Pratt did the electron microprobe analyses.

#### References

- Bayliss, P. (1968) The crystal structure of disordered gersdorffite. *American Mineralogist*, 53, 290–293.
- Bayliss, P. (1969a) X-ray data, optical anisotropism, and thermal stability of cobaltite, gersdorffite, and ullmannite. *Mineralogical Magazine*, 37, 26–33.
- Bayliss, P. (1969b) Isomorphous substitution in synthetic cobaltite and ullmannite. *American Mineralogist*, 54, 426–430.
- Bayliss, P. (1982) A further crystal structure refinement of cobaltite. *American Mineralogist*, 67, 1048–1057.
- Bayliss, P. and Stephenson, N. C. (1967) The crystal structure of gersdorffite. *Mineralogical Magazine*, 36, 38–42.
- Bayliss, P. and Stephenson, N. C. (1968) The crystal structure of gersdorffite (III), a distorted and disordered pyrite structure. *Mineralogical Magazine*, 36, 940–947.
- Berry, L. G. and Thompson, R. M. (1962) X-ray Powder Data for Ore Minerals: The Peacock Atlas. Geological Society of America Memoir, 85.
- Cabri, L. J. and Laflamme, J. H. G. (1976) The mineralogy of the platinum-group elements from some copper–nickel deposits of the Sudbury area, Ontario. *Economic Geology*, 71, 1159–1195.
- Giese, Jr. R. F. and Kerr, P. F. (1965) The crystal structures of ordered and disordered cobaltite. *American Mineralogist*, 50, 1002–1014.
- King, H. E. Jr. and Prewitt, C. T. (1979) Structure and symmetry of  $CuS_2$  (pyrite structure). *American Mineralogist*, 64, 1265–1271.
- Klemm, D. D. (1962) Anisotropieeffekte bei kubischen Erzmineralien. *Neues Jahrbuch für Mineralogie Abhandlungen*, 97, 337–356.
- Klemm, D. D. (1965) Synthesen und Analysen in den Dreieckdiagrammen  $FeAsS-CoAsS-NiAsS$  und  $FeS_2-CoS_2-NiS_2$ . *Neues Jahrbuch für Mineralogie Abhandlungen*, 103, 205–255.
- Nelson, J. B. and Riley, D. P. (1945) An experimental investigation of extrapolation methods in the derivation of accurate unit-cell dimensions of crystals. *Proceedings of the Physics Society*, 57, 160–177.
- Pratt, J. L. and Bayliss, P. (1979) Crystal structure refinement of cattierite. *Zeitschrift für Kristallographie*, 150, 163–167.
- Pratt, J. L. and Bayliss, P. (1980) Crystal structure refinement of a cobaltian ullmannite. *American Mineralogist*, 65, 154–156.
- Ramdohr, P. (1969) *The Ore Minerals and Their Intergrowths*. Pergamon Press, New York.
- Tennyson, C. (1980) Zwillingsstrukturen. *Lapis*, 5, Nr. 2, 12–14.
- Wuensch, B. J. and Prewitt, C. T. (1965) Corrections for X-ray absorption by a crystal of arbitrary shape. *Zeitschrift für Kristallographie*, 122, 24–59.
- Yund, R. A. (1962) The system Ni–As–S: phase relations and mineralogical significance. *American Journal of Science*, 260, 761–782.

*Manuscript received, July 21, 1981;  
accepted for publication, March 1, 1982.*